

**APPLICATION OF RESPONSE SURFACE
METHODOLOGY (RSM) FOR OPTIMIZATION
PARAMETER OF LSCF-CuO FOR INTERMEDIATE
TEMPERATURE SOLID OXIDE FUEL CELLS**

JONATHON JOHN

UNIVERSITI SAINS MALAYSIA

2021

**APPLICATION OF RESPONSE SURFACE
METHODOLOGY (RSM) FOR OPTIMIZATION
PARAMETER OF LSCF-CuO FOR INTERMEDIATE
TEMPERATURE SOLID OXIDE FUEL CELLS**

by

JONATHON JOHN

**Thesis submitted in fulfilment of the requirements
for the degree of
Bachelor of Chemical Engineering**

July 2021

ACKNOWLEDGEMENT

First and foremost, I would like to express my utmost gratitude to God, the great almighty who grants me with knowledge, strength, and determination to accomplish my Final Year Project research work. Next, I would also like to extend my sincere gratitude to my supervisor, Dr Noorashrina A. Hamid who has been a great support and pillar of strength throughout this research period. She also conducted a lot of online meeting to check my progress as well as clear my doubts on my title. Again, a million thanks to her for all the encouragement and endless advice she has given to me. Her immense knowledge, ideas, and vision has been the reason for this research to be completed in time and with encouraging results. Apart from them, I would like to express my hearty gratitude to the final year project coordinator, Professor Dr. Mohd Roslee Othman for his continuous supervision and precious motivation to all final year students on completing this undertaking. I also like to thank to all the Professors who had conducted online classes on how to compose literature review, help in finding relevant articles also helped in citations. Thank you.

TABLE OF CONTENT

ACKNOWLEDGEMENT.....	I
LIST OF TABLES.....	IV
LIST OF FIGURES.....	V
LIST OF FLOWCHARTS.....	VII
LIST OF ABBREVIATIONS.....	VIII
LIST OF SYMBOLS.....	IX
ABSTRAK.....	X
ABSTRACT.....	XI
1. CHAPTER 1: INTRODUCTION.....	1
1.1 Background.....	1
1.2 Problem Statement.....	5
1.3 Objectives.....	5
2. CHAPTER 2: LITERATURE REVIEW.....	6
2.1 Cathode.....	6
2.2 Polarization Resistance.....	11
2.3 Calcination Temperature.....	13
2.4 Doping effect of on perovskite cathode.....	16
2.5 Optimization using Response Surface Methodology (RSM).....	19

3. CHAPTER 3: METHODOLOGY.....	26
4. CHAPTER 4: RESULT AND DISCUSSION.....	32
4.1 Adequacy of model.....	32
4.2 Analysis of variance (ANOVA).....	42
4.3 Model Interaction.....	47
4.4 Optimization of LSCF-CuO fuel cell.....	52
4.5 Sustainability.....	57
5. CHAPTER 5: CONCLUSION AND RECOMMENDATION.....	58
5.1 Conclusion.....	58
5.2 Recommendation.....	59
REFERENCES.....	60

LIST OF TABLES

Table 1.1 : CO ₂ emissions by U.S. electric power sector by source,2020; <i>extracted from U.S. Energy -Related CarbonDioxide Emissions, 2020 (Jamieson, 2021)</i>	2
Table 2.1 : Specific surface area (m ² /g) for both sol-gel and solid-state synthesis method at different calcination temperature; <i>adapted from Physical and Chemical Properties of LSCF-CuO as potential cathode for IT-SOFC (Mohd Abd Fatah and A. Hamid 2018)</i>	14
Table 2.2 : Polarization resistance (Ω cm ²) at different sintering and operating temperature; <i>adapted from Influence of Sintering Temperature on the Polarization Resistance of LSCF-SDCC (Baharuddin et al. 2016)</i>	15
Table 3.1 : Parameters and levels for CCD, Historical data and Optimal-D.....	28
Table 3.2 : Experimental runs of CCD and response for polarization resistance.....	29
Table 3.3 : Experimental runs of historical data and response for polarization resistance.....	30
Table 3.4 : Experimental runs of D-optimal and response for polarization resistance.....	31
Table 4.1 : Model summary statistics.....	33
Table 4.2 : ANOVA test for CCD design.....	44
Table 4.3 : ANOVA test for Historical data design.....	45
Table 4.4 : ANOVA test for Optimal-D design.....	46
Table 4.5 : Model coefficient for CCD, Historical data and Optimal-D designs;A-Temperature, B-CuO concentration.....	48
Table 4.6 : Constraint set up for the optimization using the 3 designs.....	52
Table 4.7 : Summarize optimized LSCF-CuO fuel cell using CCD, Historical data and Optimal-D.....	56
Table 4.8 : Comparison of the predicted optimization with the experimental data for the 3 designs.....	56

LIST OF FIGURES

Figure 1.1 : Operating principle of a typical SOFC; <i>adapted from Solid Oxide Fuel Cell: Past Present and Future (Irvine and Connor 2013)</i>	3
Figure 2.1 : Triple-phase boundary (TPB) Region. Cathode as electronic phase (α), Oxygen as gasphase (β) and electrolyte as ionic phase (γ); <i>extracted from (P. Kaur and Singh 2020)</i> ..	7
Figure 2.2 : Typical ideal cubic perovskite structure; <i>adapted from Recent Advances of</i>	8
Figure 2.3 : a) shows the bulk oxygen transport in common perovskite structure such as LSM, b) shows the bulk oxygen transport in MIEC based cathode (LSCF); <i>extracted from Factors Governing Oxygen Reduction in Solid Oxide Fuel Cell Cathodes (Adler 2004)</i> ...	10
Figure 2.4 : Three possible path for cathodic reaction for perovskite based cathode; <i>extracted from Solid Oxide Fuel Cell Cathodes: Polarization Mechanisms and Modelling of the Electrochemical Performance (Fleig 2003)</i>	12
Figure 2.5 : Cubic representation of RSM based central composite design (CCD); <i>adapted from Response Surface Methodology (RSM) as a tool for optimization in analytical chemistry (Bezerra et al. 2008)</i>	21
Figure 2.6 : Response surface plot for discharge capacity (<i>Huang et al. 2016</i>).....	23
Figure 2.7 : Response surface plot for power density ($C_{\text{MEOH}}=1.25 \text{ M}$, $Q_{\text{O}_2}= 300 \text{ ml/min}$, and $T= 70 \text{ }^\circ\text{C}$) (<i>Sharifi et al. 2020</i>).....	24
Figure 2.8 : Response surface plot for power density ($C_{\text{MEOH}}=1.35 \text{ M}$, $\text{MOR}= 1.47\%$, and $T= 70 \text{ }^\circ\text{C}$) (<i>Charoen et al. 2017</i>).....	25
Figure 3.1 : Experimental data for optimization.....	27
Figure 4.1 Graph of predicted vs actual of he polarization resistance using CCD design.....	34
Figure 4.2 : Graph of predicted vs actual of he polarization resistance using Historical data design.....	35

Figure 4.3 : Graph of predicted vs actual of he polarization resistance using Optimal-D design.	36
Figure 4.4 : Normal probability plot for the residual from the polarization resistance model for CCD design.....	37
Figure 4.5 : Normal probability plot for the residual from the polarization resistance model for Historical data design.....	38
Figure 4.6 : Normal probability plot for the residual from the polarization resistance model for Optimal-D design.....	39
Figure 4.7 : Internally studentized residual vs predicted response for the polarization resistance for CCD design.....	40
Figure 4.8 : Internally studentized residual vs predicted response for the polarization resistance for Historical data design.....	41
Figure 4.9 : Internally studentized residual vs predicted response for the polarization resistance for Optimal-D design.....	42
Figure 4.10 : Contour plot for the polarization resistance using Optimal-D design.....	49
Figure 4.11 : 3D interaction plot for the polarization resistance using Optimal-D design.....	50
Figure 4.12 : Optimum sintering condition of cathode using CCD design.....	53
Figure 4.13 : Optimum sintering condition of cathode using Historical data design.....	54
Figure 4.14 : Optimum sintering condition of cathode using Optimal-D design.....	55

LIST OF FLOWCHARTS

Flowchart 2.1 : Steps involved in conducting design expert (DOE); <i>extracted from Handbook 151: NIST/SEMATECH e-Handbook of Statistical Methods(Heckert et al. n.d.).</i>	20
Flowchart 3.1 : Flowchart of the simulation of experimental design based response surface methodology(RSM).....	26

LIST OF ABBREVIATIONS

Symbol	Description
SOFC	Solid oxide fuel cell
HT-SOFC	High temperature solid oxide fuel cell
IT-SOFC	Intermediate temperature solid oxide fuel cell
DMFC	Direct methanol fuel cell
MIEC	Mixed ionic electronic conductor
LSCF	Lanthanum strontium cobalt ferrite
LSM	Lanthanum strontium manganite
BSCF	Barium strontium cobalt ferrite
CuO	Copper (II) oxide
ORR	Oxygen reduction reaction
ASR	Area-specific resistance
TPB	Triple phase boundary
DOE	Design of experimental
RSM	Response surface methodology
CCD	Central composite design
ANOVA	Analysis of variance
CV	Coefficient of variation
PRESS	Predicted residual error sum of square
df	Degree of freedom

LIST OF SYMBOLS

Symbol	Description	Unit
R_p	Polarization resistance	Ωcm^2
O^{2-}	Oxygen gas ion	-
α	Electron phase	-
β	Gas phase	-
γ	Ion phase	-
β_i	Linear coefficient	-
β_0	Constant coefficient	-
β_{ii}	Quadratic coefficient	-
β_{ij}	Linear model interaction coefficient	-

**PEMAKAIAN RESPONSE SURFACE METODOLOGI (RSM) UNTUK
PENGOPTIMUMAN PARAMETER LSCF-CuO UNTUK INTERMEDIATE
TEMPERATURE OKSIDA SOLID SEL FUEL**

ABSTRAK

Pengoptimuman ferit lanthanum strontium kobalt dicampur dengan tembaga (II) oksida (LSCF-CuO) untuk keadaan sintesis dilakukan untuk memaksimumkan prestasi bahan bakar. Pengoptimuman dilakukan dengan menggunakan Metodologi Permukaan Respons; Reka bentuk komposit pusat (CCD), data Sejarah dan model Optimal-D dalam perisian Design-Expert (12) dan perbandingan antara keduanya telah dibuat. Pengoptimuman dilakukan melalui eksperimen yang telah dilakukan untuk menganalisis parameter, suhu sintering ($^{\circ}$ C) dan kepekatan CuO (wt%) pada rintangan polarisasi Ωcm^{-2} yang secara tidak langsung mempengaruhi prestasi sel bahan bakar. Analisis kecukupan untuk ketiga-tiga reka bentuk menunjukkan plot taburan normal yang menunjukkan ketepatan kuadratik untuk meramal tindak balas. Berdasarkan analisis ANOVA untuk ketiga-tiga reka bentuk, nilai p kurang dari 0,05 untuk suhu sintering dan kepekatan CuO menunjukkan pengaruh yang signifikan dari parameter ini pada rintangan polarisasi. Berdasarkan analisis ringkasan yang sesuai, reka bentuk menunjukkan kesesuaian model kuadratik kerana R^2 untuk CCD, data Sejarah dan Optimal-D masing-masing adalah 0,9911, 0,9936 dan 0,9959 (dekat dengan kesatuan). Tujuan pengoptimuman adalah untuk meminimumkan rintangan polarisasi dan oleh itu model Optimal-D menunjukkan hasil pengoptimuman yang baik kerana ia menunjukkan R_p terendah $0,11 \Omega\text{cm}^{-2}$ dibandingkan dengan data Sejarah ($0,16 \Omega\text{cm}^{-2}$) dan CCD ($0,12 \Omega\text{cm}^{-2}$). Suhu sintering yang optimum dan kepekatan CuO untuk Optimal-D masing-masing adalah 656° C dan 1.65 wt%.

**APPLICATION OF RESPONSE SURFACE METHODOLOGY (RSM) FOR
OPTIMIZATION PARAMETER OF LSCF-CuO FOR INTERMEDIATE TEMPERATURE
SOLID OXIDE FUEL CELLS**

ABSTRACT

Optimization of lanthanum strontium cobalt ferrite mixed with copper (II) oxide (LSCF-CuO) for the synthesis condition is carried out to maximize the fuel performance. The optimization is carried out using Response Surface Methodology; Central composite design (CCD), Historical data and Optimal-D models in the Design-Expert (12) software and the comparison between them have been made. The optimization was carried over a done experiment to analyze the parameters, sintering temperature ($^{\circ}\text{C}$) and CuO concentration (wt%) on the polarization resistance Ωcm^{-2} which indirectly affect the fuel cell performance. The adequacy analysis for all the 3 designs shows normal distribution plot which indicate the accuracy of the quadratic to predict the response. Based on ANOVA analysis for all the 3 designs, p value of less than 0.05 for the sintering temperature and CuO concentration indicate a significant effect of these parameters on the polarization resistance. Based on the fit summary analysis, the designs shows good fit of quadratic models since the R^2 for CCD, Historical data and Optimal-D are 0.9911, 0.9936 and 0.9959 respectively (close to unity). The aim of the optimization is to minimize the polarization resistance and therefore Optimal-D model shows the good optimization result since it exhibit the lowest R_p of $0.11 \Omega\text{cm}^{-2}$ compared to Historical data ($0.16 \Omega\text{cm}^{-2}$) and CCD ($0.12 \Omega\text{cm}^{-2}$). The optimized sintering temperature and CuO concentration for Optimal-D were 656°C and 1.65 wt % respectively.

1. CHAPTER 1: INTRODUCTION

1.1 Background

The global energy demand is increasing with the economic growth combined with the steadily rising population. John Sheffield claims that the world energy would be raised to 15,000 to 21,000 Mega tonnes of equivalent oil per year by the time the world population has risen from 6 billion to around 12 billion people in the 22nd century (Sheffield 1998). The most preferred source of energy for electrical generation would be the non-renewable sources since it has better efficiency and cost effective compared to renewable sources. According to Statistical Review of World Energy and Ember 2019, the major contribution of electrical energy production worldwide by coal and natural gas are 36.38 % and 23.32% respectively (BP, 2020). The dependency on fossil fuel such as coal and natural gas for electrical power generation would be a major issue since they will be depleted soon. According to world data, the fossil fuel reserve depletion time for oil, natural gas and coal are approximately 50.7, 52.8 and 114 years respectively (Ritchie & Roser, 2017) . These statistical data is based on constant rate of production based on year 2015 as the reference. These energy sources becomes a greater challenge now and in future due to its raw material availability and emission of greenhouse gases. U.S. Energy Information Administration (EIA) reported that emission of greenhouse gases typically carbon dioxide (CO₂) by U.S electric power sector were 1618 million metric tons (MMmt) which is around 31 % of total U.S. energy-related CO₂ emission. Coal and natural gas are the main cause of the emission of greenhouse gases typically CO₂ from the generation of electricity and thus lead to environmental issues such as global warming and climate changes. Since these coal and natural gas are being limited as mentioned earlier, thus a more sustainable and clean energy source to produce electricity is preferred.

Table 1.1 : CO₂ emissions by U.S. electric power sector by source,2020; *extracted from U.S. Energy -Related CarbonDioxide Emissions, 2020 (Jamieson, 2021).*

Source	Million metric tons	Share of sector total (%)
Coal	786	54
Natural gas	635	44
Petroleum	16	1
Other	11	<1

Solid oxide fuel cell (SOFC) becomes an emerging technology replacing the fossil fuel due to its production of clean energy that is more sustainable and environmentally friendly. SOFC have certain design that is more reliable energy source such as high energy efficiency compared to conventional power plants, fuel flexibility and absence of corrosive liquids (Shao and Halle 2004). SOFC utilizes the concept of electrolysis. It consists of electrodes known as cathode and anode and a media to transfer the electrical charge which is known as the electrolyte. The fuel cell converts chemical energy into electrical energy through a series of electrochemical reaction without any occurrence of combustion (Stambouli and Traversa 2002). A typical illustration of the working mechanism for the SOFC is shown in **Figure 1.1** below.

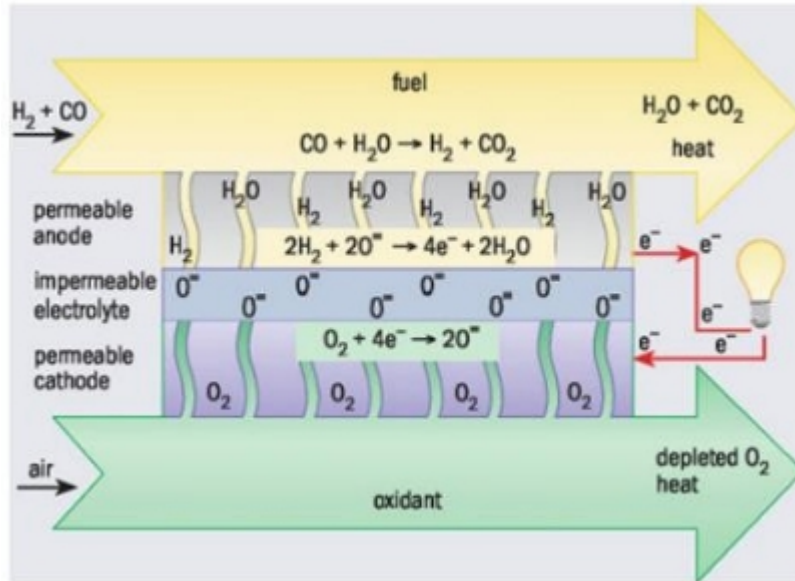


Figure 1.1: Operating principle of a typical SOFC; adapted from *Solid Oxide Fuel Cell: Past Present and Future*(Irvine and Connor 2013).

Fuel cells distribute high electrical conversion efficiency compared to coal-fired power plant due their efficiency is not limited by the Carnot efficiency because the electrical work is directly converted from the enthalpy associated with the electrochemical oxidation into water and carbon dioxide (Irvine and Connor 2013). This high efficiency of SOFC requires only less fuel being consumed to generate a certain amount of electricity which directly implies of lower emission of carbon dioxide CO_2 , the main ‘greenhouse gases’ responsible for global warming. Besides that, emission of SOFC system will be low nearly zero level of NO_x and SO_x , which is accountable for acid rain formation (Stambouli and Traversa 2002) .

Several studies have been conducted on commercializing the SOFC technology in generating electricity. In Japan, a group of companies consist of Osaka Gas Co. Ltd, Aisin Seiki Co. Ltd, Kyocera Corporation, Chofu Seisakusho Co. Ltd and Toyota Motor Corporation have developed SOFC cogeneration system to supply power to residential areas. The product which is also known as “ENE-FARM Type S” utilizes the ceramic electrolyte to generate power which operate at high

operating temperature around 700-750 °C. This product achieved highest level of power generation efficiency worldwide which is around 46.5%. It also estimated to supply 80% power needed in a particular household (“Japanese Group Unveils SOFC Ene-Farm Residential Cogen Unit” 2012). SOFC consists of electrode (cathode and anode), electrolyte, sealing material, interconnects, and stack design arrangement (planar and tubular)(Irshad et al. 2016). Since our focus is the synthesis of the type of electrode typically cathode thus the other parameters are not discussed in detail.

The classification of SOFC is based on operating temperature and electrolyte material used. Usually, the SOFC will be operated at very high temperature (HT-SOFC) around 850 °C - 1000 °C for the power generation intention (M. Kaur, Kaur, and Kumar 2019). However, operating at high temperature may reduce the durability of the fuel cell and the cost for electrode materials used at higher temperature typically ceramics are expensive (Combemale, Sivasankaran, and Caboche 2016). To overcome this problem, the SOFC will be operated at low or intermediate temperature (IT-SOFC) around 500 °C - 750 °C. IT-SOFC has wider benefits compared to HT-SOFC such as reduced start-up time, less vulnerable to mechanical and thermal stresses, wide range of material selection for cathode, reduction on corrosion rate and most importantly extensive range for the improvement of the reliability of the fuel cell (M. Kaur, Kaur, and Kumar 2019).

1.2 Problem Statement

Operating condition of SOFC is very crucial especially in the performance of the fuel cell. Many fuel cells operate at high temperature due to higher temperature enhances the oxygen reduction reaction (ORR). Since the activation energy is directly proportional to temperature, thus the particle will have more energy at high temperature thereby increases the rate of oxygen reduction process. However, conventional electrode such as LSCF typically will not function at very high temperature since, their durability will decrease and thus in the end lost their functionality as well. Several studies shows that use of ceramic based cathode would be the solution for this problem. However, the ceramic based electrode is very expensive. Reducing the temperature to low or intermediate, will decrease the performance of the ORR as well. Therefore, the existing SOFC typically LSCF based cathode undergo certain modification such as doping to enhance the ORR at intermediate temperature. In this work, we will focus on the optimization of the parameters that effect the ORR of LSCF-CuO based electrode which is the calcination temperature and a concentration of CuO doping element. The optimization is carried out using the central composite design (CCD), historical data and optimal-D in RSM. The optimization result will be compared within the 3 types of optimization method.

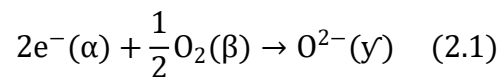
1.3 Objectives

1. To optimize the parameters which are calcination temperature of doped electrode and concentration of CuO on the polarization resistance using the CCD, historical data and optimal D in RSM.
2. To compare and contrast among the 3 optimization methods.

2. CHAPTER 2: LITERATURE REVIEW

2.1 Cathode

The reduction of oxygen gas into (O^{2-}) ions occurs at the cathode which is shown in equation (2.1) below (Elleuch and Halouani 2019). To have better oxygen reduction process, the cathode must have high electronic conductivity, chemical stability, compatible thermal expansion, least reactivity with the electrolyte, high catalytic activity for oxygen molecules dissociation and stable porous microstructure to ease the diffusivity of oxygen from cathode into electrolyte interface (Anon 1986). As notice in equation(2.1), the gas phase oxygen will diffuse into the porous structure of the cathode and get reduced into O^{2-} at the interface of cathode and electrolyte (α/γ interphase). Since this reaction involve ions, electrons and gas molecules in three separate phases, the α/γ interphase in contact with the gas phase, β is known as three-phases boundary (TPB)(Adler 2004). The electrochemical reaction at cathode occurs at the TPB region only and this reduction process contribute to the overall resistivity of the cells and this TPB region also determine the overall performance of fuel cells. The length of TPB region is directly proportional to the cell performance whereby larger TPB enhances the reduction of the oxygen into ions(P. Kaur and Singh 2020). In recent years, many approaches have been done and carried out to increase the length of TPB region using different cathode materials. **Figure 2.1** shows a typical illustration of the oxygen reduction reaction (ORR) at the TPB.



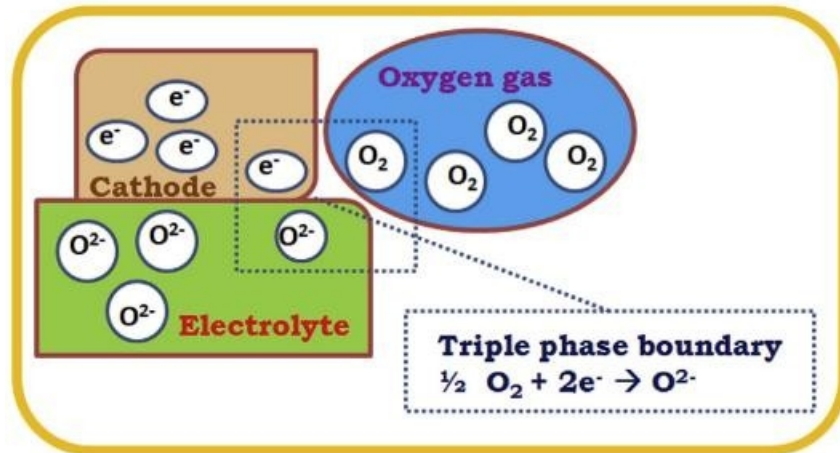


Figure 2.1: Triple-phase boundary (TPB) Region. Cathode as electronic phase (α), Oxygen as gasphase (β) and electrolyte as ionic phase (γ); extracted from (P. Kaur and Singh 2020)

Conventionally, porous platinum (Pt), palladium (Pd) and gold (Au) based cathode which is known as noble metals is being used for the SOFC. Pt based cathode is rarely used as cathode materials since it is costly and also have larger resistivity which is also known as polarization resistance which will be discussed later (Riedl et al. 2020). Later years, the use of perovskites oxides replacing the expensive Pt cathode have been researched. The structure of perovskite oxides is closely related to the enhancement of the cathode material. Thus, a brief description of the structure enables us to understand the theoretical explanation for the better cathode performance.

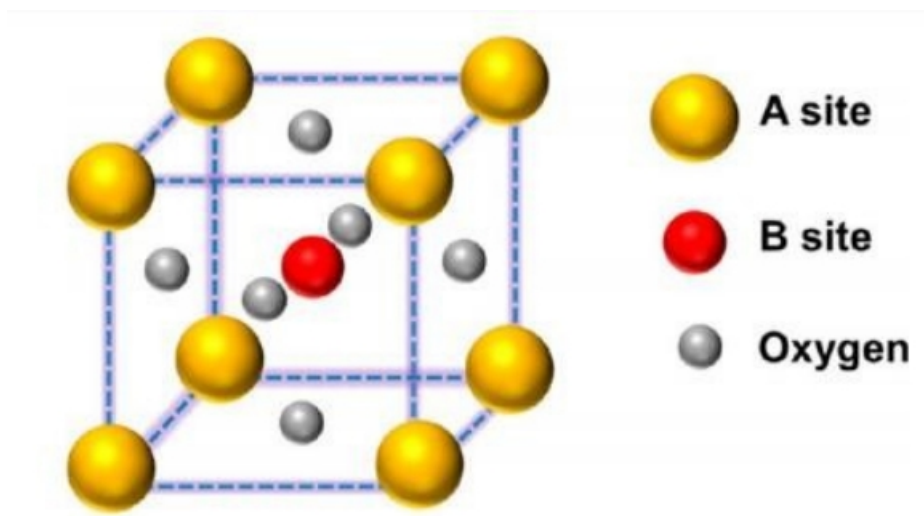


Figure 2.2: Typical ideal cubic perovskite structure; *adapted from Recent Advances of Lanthanum -Based Perovskiteoxides for Catalysis (Zhu, Zhang, and Dai 2015).*

The general formula for this perovskite structure is ABO_3 . The corners of the cubic structure occupied by A-site cations which is known as alkali earth metals. Some of the examples of these metals are strontium (Sr), barium (Ba), lanthanum (La), praseodymium (Pr), Neodymium (Nd) and Calcium (Ca). The B-site cation is known as transition metals which will be located at the centre of the cubic structure. Examples of the B-site cations are titanium (Ti), manganese (Mn), ferrite (Fe), cobalt (Co) and copper (Cu) (P. Kaur and Singh 2020). The octahedral symmetry around the B-site cations assist in metallic or semiconducting band structure at high temperature which promote high electronic conduction at the cathode. Proper choices of cations for A-site and B-site would increase the quantity of stable oxygen ion vacancies which promote significant bulk oxygen transport and thus the ORR rate of reaction would be enhanced. (Adler 2004).

Early stage of perovskite oxide, lanthanum strontium manganite (LSM) based cathode were used. Strontium is used as the doping element for lanthanum manganite since the size is compatible with the lanthanum (Ralph, Schoeler, and Krumpelt 2001). The electronic conductivity of the LSM

rises as the concentration of the Sr increases at a maximum mol of 50%. LSM shows good performance at high operating temperature around 1000 °C (Sun, Hui, and Roller 2010). At lower temperature or intermediate temperature, there is no vacancy for oxygen in the ABO₃ perovskite structure. This will cause the oxygen reduction reaction to be restricted at the TPB (Ralph, Schoeler, and Krumpelt 2001). This would be the main reason LSM based cathode are not suitable to be used at lower temperature since it has low ionic conductivity and slow surface oxygen exchange kinetics (Irvine and Connor 2013). Studies have been conducted to increase the performance of LSM cathode at lower temperature in 2 main methods which is extending surface area for ORR which is the TPB region by adding second ionically conducting phase to LSM. The second method is by replacing the A-site cations which is initially occupied by lanthanum to any other alkali earth metal to promote the formation of oxygen vacancies (Ralph, Schoeler, and Krumpelt 2001).

To enhance the properties such as ionic and electronic conductivity of the cathode at low or intermediate temperature, mixed ionic and electronic conductor (MIEC) cathode material is being synthesis and preferred. MIEC material originated from the perovskite oxide structure (ABO₃) which was shown in **Figure 2.2** above (Burnwal, Bharadwaj, and Kistaiah 2016). The design of MIEC cathode with a single chemical composition consist of lanthanum at the A-site and combination of transition metals such as cobalt, ferrite or/and nickel on the B-site (Gellings et al. 1997). The partial substitution of A-site cations increases the oxygen vacancies in the system. As a result, the cathode material will have enhanced ionic conductivity to maintain the electrical neutrality caused by the oxygen vacancies. The use of mixed components in B-site will affect the concentration of the oxygen vacancies. Overall, the cathode will have high ionic conductivity due to high concentration of oxygen vacancies and good electronic conductivity due to mixed-valence state of different components in B-site (cobalt and ferrite) (Gellings et al. 1997). Operating at

lower or intermediate temperature will eventually lead to slower kinetic of ORR since the temperature is directly proportional to the rate of reaction based on the Arrhenius equation (Burnwal, Bharadwaj, and Kistaiah 2016). The rule of thumb needs to consider would be the increasing the active area for the reaction to occur or increasing the length of TPB to enhance the cell performance. MIEC based cathode also promote simultaneous transport of both ionic and electronic species thus, increasing the size of possible reaction sites (Adler 2004). A typical illustration for the transport of bulk oxygen in normal perovskite oxide and MIEC based cathode is shown in **Figure 2.3** below. This is a one of the most important criteria since the ORR will not be limited at the TPB region which was discussed earlier for LSM cathode. In other words, the ORR reaction occurs throughout the entire surface of the cathode (Burnwal, Bharadwaj, and Kistaiah 2016). The promising MIEC cathode materials that have been researched and used commercially are lanthanum strontium cobalt ferrite (LSCF) and barium strontium cobalt ferrite (BSCF).

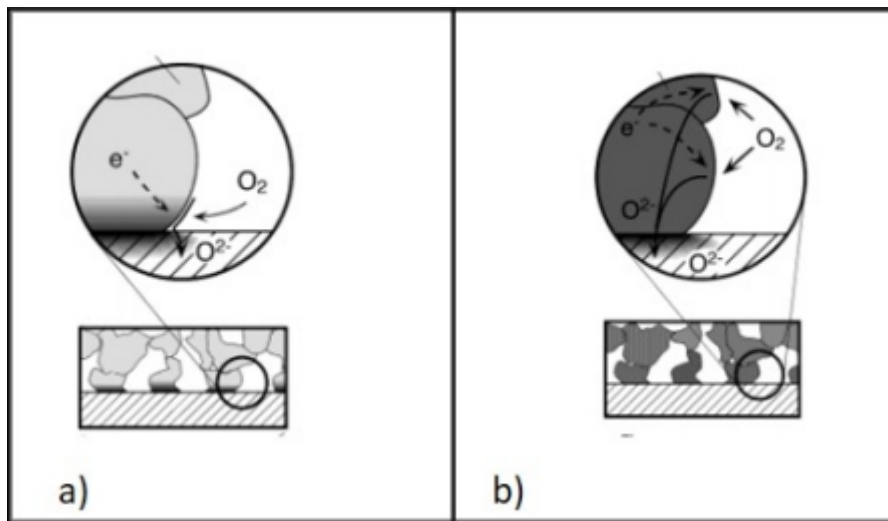


Figure 2.3: a) shows the bulk oxygen transport in common perovskite structure such as LSM, b) shows the bulk oxygen transport in MIEC based cathode (LSCF); *extracted from Factors Governing Oxygen Reduction in Solid Oxide Fuel Cell Cathodes (Adler 2004)*

2.2 Polarization Resistance

Polarization resistance seems to be insignificant at higher operating temperature, since higher temperature promote high activation energy thus, reducing the polarization resistance. However, SOFC operating at low or intermediate temperature, polarization resistance become dominant in the overall performance of the cathode. As discussed earlier, the ORR happens at the TPB which was mentioned in earlier section. Perovskite oxides-based cathode have three possible routes for the reaction to occur which are electrode surface path, bulk path and lastly electrolyte surface path. The electrode surface path consists of diffusion of oxygen gas, adsorption of oxygen onto the electrode surface and finally diffusion of oxygen to the TPB region. The bulk path includes oxygen gas diffusion, adsorption on the perovskite oxide cathode surface, dissociation and ionization, incorporation into the cathode, oxide ion transport and transport of ion into the electrode. The last pathway which is the electrolyte surface path include oxygen diffusion, adsorption, and ionization on the electrolyte surface. For all the pathways mentioned, there will be one or more elementary steps that determine that become the rate determining step which end up becomes the overall reaction rate. The resistance is not only present from these pathways but for the flow of electrons from current collector to the electron-consuming active site also need to be considered as well. **Figure 2.4** below shows graphical representation of the three pathways involved during cathodic reaction. Much research has been in progress to reduce the polarization resistance of cathode to improve the cell performance such as adding doping elements to the existing perovskite structure to increase the TPB region area. The effect of doping elements on the polarization resistance will be discussed in next section. The focus of our paper would be the effect of varied doping concentration with the MIEC based cathode which is LSCF and effect of sintering or calcination temperature of these cathode. Both factors are

related to the particle size distribution of the fabricated cathode and thereby contribute to the polarization resistance as well.

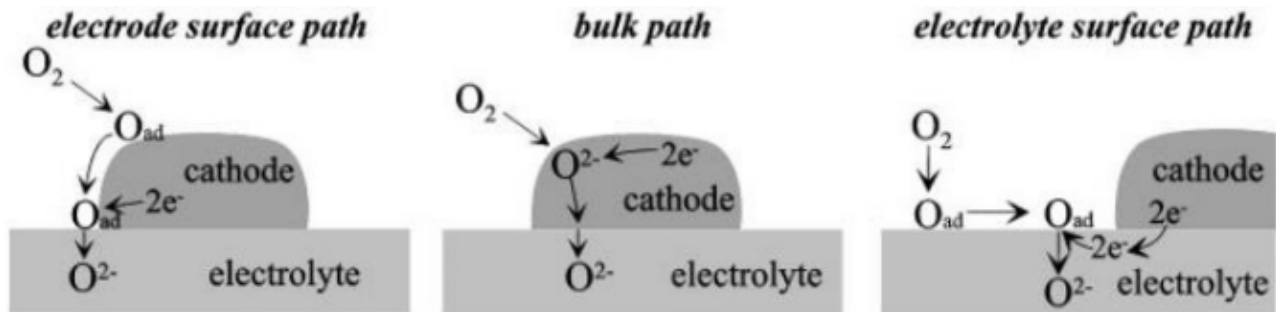


Figure 2.4: Three possible path for cathodic reaction for perovskite based cathode; extracted from *Solid Oxide Fuel Cell Cathodes: Polarization Mechanisms and Modelling of the Electrochemical Performance* (Fleig 2003).

2.3 Calcination Temperature

Generally, increasing the calcination temperature would increase the size of microstructure of the cathode. This will result in decrease the surface area of gas-solid interphase (TPB region) due to decrease in porosity which result in high polarization resistance(Baharuddin et al. 2016). On the other hand, if the sintering temperature is too low, it may lead to insufficient sintering which causes poor adhesion of the cathode component to the electrolyte thus, this result in poor performance of the SOFC(Baharuddin et al. 2018). Due to these reasons, sintering temperature become a crucial parameter in determine the lowest polarization resistance for better cell performance.

Ahmad Fuzamy investigated the effect synthesis routes of the LSCF doped copper (II)oxide (CuO) an the calcination temperature on the performance of the IT-SOFC (Mohd Abd Fatah and A. Hamid 2018). The electrodes were prepared using sol-gel route and solid-state route at different calcination temperature. It was found that the sol-gel route produces larger surface area LSCF-CuO samples compared with the solid-state route using the BET (Brunauer–Emmett–Teller) analysis which is shown in **Table 2.1** below. Larger surface area indicates that the microstructure of LSCF-CuO synthesized from sol- gel method is smaller than solid state method. As the temperature increases, the specific surface area also decreases. The decreased in surface area indicate larger particle size which indicate larger polarization resistance.

Table 2.1: Specific surface area (m^2/g) for both sol-gel and solid-state synthesis method at different calcination temperature; *adapted from Physical and Chemical Properties of LSCF-CuO as potential cathode for IT-SOFC (Mohd Abd Fatah and A. Hamid 2018).*

Method	Temperature °C	Specific Surface area (m^2/g)
sol-gel	600	11.0465
	700	8.1583
	800	4.1716
	900	1.8114
solid-state	600	13.3265
	700	4.5542
	800	3.2195
	900	1.4704

Another study was conducted by Nurul Akidah Baharuddin on the influence of sintering temperature on the polarization resistance of LSCF composite with samarium-doped ceria carbonate (SDCC)(Baharuddin et al. 2016). The composite cathode was prepared in an equal weight% composition (50 wt% LSCF-50 wt% SDCC). The range of sintering temperature used are from 550 °C to 750 °C. The first analysis was made to analyse the performance of cathode using the size of grain. As the sintering temperature increases, the average surface porosity decreases. The decrease in porosity surface is associated with increasing grain size. This causes the polarization resistance to increase as larger grain size have smaller specific surface area thus decreasing the oxygen reduction reaction. The result was supported with the theoretical explanation whereby high sintering temperature promote the formation of large microstructure. As we can see from **Table 2.2**, the polarization resistance increases with increasing calcination temperature. However, it should take note that operating temperature is totally different from calcination temperature. The effect of operating temperature was explained earlier whereby higher operating temperature increases the activation energy for ORR to occur thus enhances the cell

performance. This is the reason the polarization resistance decreases with increasing operating temperature at constant sintering temperature.

Table 2.2: Polarization resistance ($\Omega \text{ cm}^2$) at different sintering and operating temperature; adapted from *Influence of Sintering Temperature on the Polarization Resistance of LSCF-SDCC* (Baharuddin et al. 2016).

Sintering Temperature ($^{\circ}\text{C}$)	Average Surface Porosity (%)		
550	31.33		
600	25.89		
650	24.33		
700	19.25		
750	12.98		

Polarization resistance ($\Omega \text{ cm}^2$)			
Sintering Temperature ($^{\circ}\text{C}$)	550	600	650
Operating Temperature ($^{\circ}\text{C}$)			
450	4.09	3.15	4.71
500	2.76	2.43	3.68
550	2.28	1.34	3.49
600	1.29	1.15	3.42
650	1.21	0.68	1.61

2.4 Doping effect of on perovskite cathode

In this study, the focus is on the doping of transition metal oxide copper (II) oxide (CuO) with our LSCF cathode and their respective performance in term of polarization resistance is analysed. However, doping of other elements such as SDC and CGO are discussed in later section. The addition of CuO will not only increase the electro-catalytic activity but it also capable to reduce the calcination temperature (Lu et al. 2012).

Lihua Lu conducted an experiment to study the effect of CuO mol % on the polarization resistance for LSCF-SDC cathode. The mole of CuO was varied from 0 % to 3 %. They found out that the ASR value initially decreases as the concentration of CuO increased from 0 to 2 mole %. This shows us that the cathodic reaction increases with CuO content which promote the decrease of polarization resistance for ORR. However, increasing the mole % of CuO beyond 2 will result in increase of polarization resistance. This is because CuO is a poor conductor of electricity thus, too much addition of CuO will become unfavourable to the charge transfer that occurs at the TPB. They concluded that 2 mol % of CuO would be the optimum concentration for promising LSCF-SDC-CuO cathode material synthesis. Based on their result, ASR value for 2 mol % CuO doping is around $0.05 \Omega \cdot \text{cm}^2$ while the ASR value of LSCF-SDC without any doping of CuO is $0.0835 \Omega \cdot \text{cm}^2$ (Lu et al. 2012).

Since our major focus is MIEC perovskite oxide-based cathode typically LSCF, thus only LSCF based doping will be discussed in detail with their respective polarization resistance. The goal to dope an existing LSCF cathode would be to reduce the polarization resistance by producing a nano-sized or micro-sized microstructure. Laura Baque mentioned from his findings that at intermediate temperature SOFC, the cathode performance is strongly depend on the microstructure (particle size, pore size or tortuosity). Thus, tiny particle size will have larger

surface area thereby increasing the region for TPB thus the rate of ORR enhanced (Baqué et al. 2008).

A study was conducted by Feng Zhou on the effect of cerium as the doping element on the performance of LSCF cathode at IT-SOFC (Zhou et al. 2018). Three electrodes were synthesized using the sol-gel method, one act as the reference (LSCF only) and the other two have cerium with different concentration $\text{La}_{0.57}\text{Ce}_{0.03}\text{Sr}_{0.4}\text{Co}_{0.2}\text{Fe}_{0.8}\text{O}_3$ (LCSCF03) and $\text{La}_{0.54}\text{Ce}_{0.06}\text{Sr}_{0.4}\text{Co}_{0.2}\text{Fe}_{0.8}\text{O}_3$ (LCSCFO6). The polarization resistance (RP) of LSCF, LCSCFO3 and LCSCFO6 are $0.21 \Omega \cdot \text{cm}^{-2}$, $0.14 \Omega \cdot \text{cm}^{-2}$ and $0.09 \Omega \cdot \text{cm}^{-2}$ respectively. We may conclude that as the concentration of cerium increases, the polarization resistance decreases due to formation of nano-scaled microstructure.

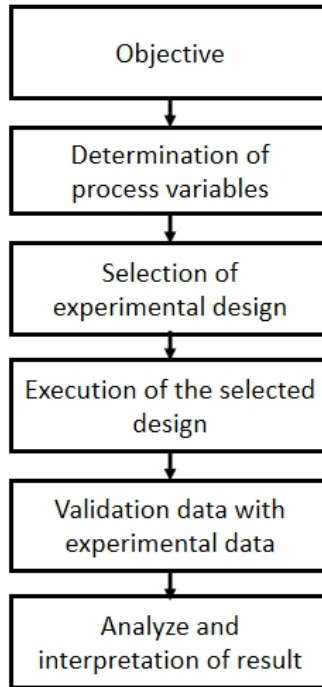
Lihua Lu carried out an experiment on the LSCF based cathode at intermediate temperature using nickelates, Ln (La_2NiO_4) as the doping materials (Lu et al. 2010). Ln shows low thermal expansion coefficient and high ionic conductivity at intermediate temperature which make it compatible for LN-LSCF cathode material. Based on his finding he found out that the area specific resistance (ASR) decreases and later increases with the calcination temperature. The ASR for lower calcination temperature around 1100°C for 30 wt% Ln is around $0.14 \Omega \cdot \text{cm}^2$ is due to poor contact between cathode and electrolyte and thus lead to increasing the resistance. Meanwhile, the ASR for higher calcination temperature (1200°C) for 30 wt% Ln is around $0.2 \Omega \cdot \text{cm}^2$ due to increase in size of microstructure at high temperature. Thus, he concluded that Ln-LSCF synthesized with 30 wt% Ln at 1150°C would be the promising cathode since it has ASR of $0.125 \Omega \cdot \text{cm}^2$.

Wei Guo Wang and Mogens Mogensen investigated the performance of composite cathode of LSCF doped CGO (cerium-gadolinium oxide) at different wt% of CGO (Wang and Mogensen

2005). They concluded that 50 wt% of CGO have lower polarization resistance compared to 30 wt% of CGO. By taking 600 °C as the operating temperature, the polarization resistance for 50 wt% CGO and 30 wt% CGO are 0.19 Ω cm² and 0.29 Ω cm², respectively.

2.5 Optimization using Response Surface Methodology (RSM).

RSM utilizes the statistical and mathematical method to analyse the response that have been affected by several variables which is known as independent variables (Bezerra et al. 2008). This design is also capable of analysing the interaction between the variables with only little number of tests run required. The main objective of RSM is optimize multivariable concurrently to achieve optimal performance of the system. The input variables are called independent variables which are controllable while the outputs are called responses. The design of RSM will be conducted using the design expert software. To obtain the design model several steps need to be followed which is shown in **Flowchart 2.1** below(Heckert et al. n.d.) . The objective of the design probably setting target for the response or to obtained maximized or minimize response. For instance, the goal to optimize fuel cell either to maximize power density or minimize the polarization resistance. Selection of process variables that significantly effect the response must be added into the list. However, if the variables are not determined as significant parameters from experimental, RSM could be used to analyse the significant parameters that effect the responding variables. The next step would be selecting proper experimental design. There are 2 categories designs in DOE software which are standard design and custom design. Usually, CCD and Box-Behnken under the category of standard design will be use for optimization. However, computer aided design such as D-optimal and I-optimal and historical data may be used as well depending on the criteria of the parameters involved. Next, the design is executed to obtained the equation of the models. In analysis of RSM, there are 3 types of model which are first order,second order and mixture models. After execution, the predicted data will be compared with the experimental data to analyse the accuracy of the model with the experimental data. Finally analysis of variance (ANOVA) test is conducted to analyses the signification of the model and also the process parameters (input variables) towards the response.



Flowchart 2.1: Steps involved in conducting design expert (DOE); *extracted from Handbook 151: NIST/SEMATECH e-Handbook of Statistical Methods(Heckert et al. n.d.).*

CCD is an experimental design for building a second order quadratic model for the response variable without the need to use a complete three-level factorial experiment. CCD consist of three different points which are axial point, cube point and centre point. Centre point are experimental run which value of the factors is the median of the factorial values, whereas the axial points are like experimental run, but the value are both higher and lower of the median of the factorial levels. The cube points are set up for the highs and lows of each factors. CCD can accurately predict the effect of independent variables and overall errors by applying minimum number of runs and able to identify important parameters from various factor(Chelladurai et al. 2020) . The CCD model is illustrated in cubical form which is shown in **Figure 2.5** below.

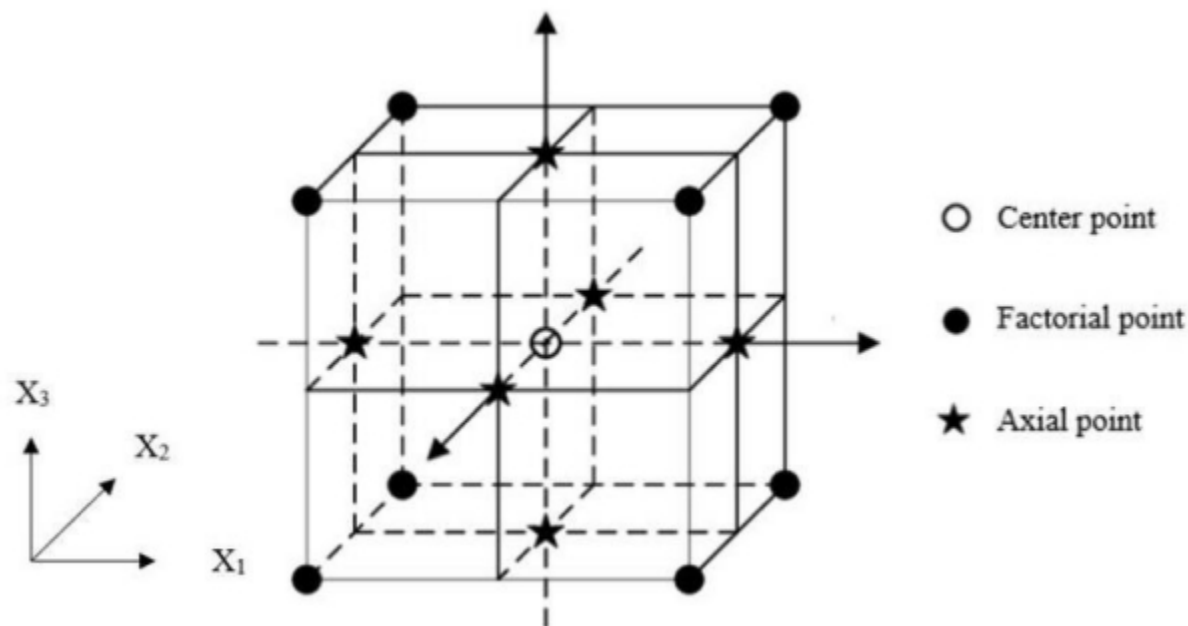


Figure 2.5: Cubic representation of RSM based central composite design (CCD); *adapted from Response Surface Methodology (RSM) as a tool for optimization in analytical chemistry (Bezerra et al. 2008)*

The historical data design was used for model development and analyse the interaction among the variables (Hooper 1993). This design enables importation of factor setting and responses of an existing experimental data to a blank design layout. In this design, the experimental data whether all or some of it will be used to define the design points (Jeirani et al. 2013).

D-optimal design is considered simpler and more feasible compared to other design method in RSM since it only requires a smaller number of tests runs than other design (Pattanaik and Rayasam 2018). This design is a computer aided design whereby it maximizes the specified information matrix of the variables involved (Holm, Jensen, and Sonnergaard 2006). This design has a major advantage compared to other type of design as it able to fit any type of mathematical model (first order, quadratic and cubic) and for any type of research field. D-optimal usually used in pharmaceutical industry for the formulation of emulsion (Ranade and Thiagarajan 2017).

Several studies have been made on the optimization of the fuel cell using CCD and historical data to obtain the desired power density. Optimization of the parameters for SOFC using central composite design (CCD) based RSM were conducted by Ismet Tikiz and Imdat Taymaz in their literature (Tikiz and Taymaz 2016). They focus on the optimization of cell temperature and the flow rates of several gases (hydrogen, oxygen, and nitrogen) towards the performance SOFC. In their case, the independent variable will be the temperature and flow rate of oxygen, flow rate of hydrogen and flow rate of nitrogen while the dependent variable is power density. It was found that the main parameters that effect the power density are cell temperature and also hydrogen flow rate. Increasing the flow rate of oxygen and nitrogen does not have significance change on the power density which is related to the performance of the cell. They concluded that the maximum power density observed from the RSM is 573.43 mW/cm^2 . This data is obtained when the flow rate of hydrogen and oxygen are 0.96 L/min and 0.98 L/min respectively and at cell temperature of $772.57 \text{ }^\circ\text{C}$.

In another literature, Xiaopeng Huang conducted a simulation using CCD to optimize the synthesis parameter of olivine-type lithium iron orthophosphate cathode (LiFePO_4) (Huang et al. 2016). This cathode have better advantage in term of high energy density and good thermal stability. However, this cathode will be doped with other element to enhance the electronic conductivity. In his literature he doped the LiFePO_4 with magnesium (Mg) and titanium (Ti). The goal of his research is to maximize the discharge capacity. Three independent variables affects the power density which are concentration of the Mg (wt%), concentration of Ti (wt%) and sintering temperature of the cathode. The result of the design shows that all the three parameters have significant effect on the response (discharge capacity). The predicted R^2 is close to actual R^2 which indicate a more precision of the obtained model using this design. The maximum power discharge obtained was 136.7 mAh/g at the operating parameter of; 2.9 wt% of Mg-dopant, 3.0

wt% of Ti-dopant and sintering temperature of 678.5 °C. The discharge capacity 3D interaction plot have been displayed in

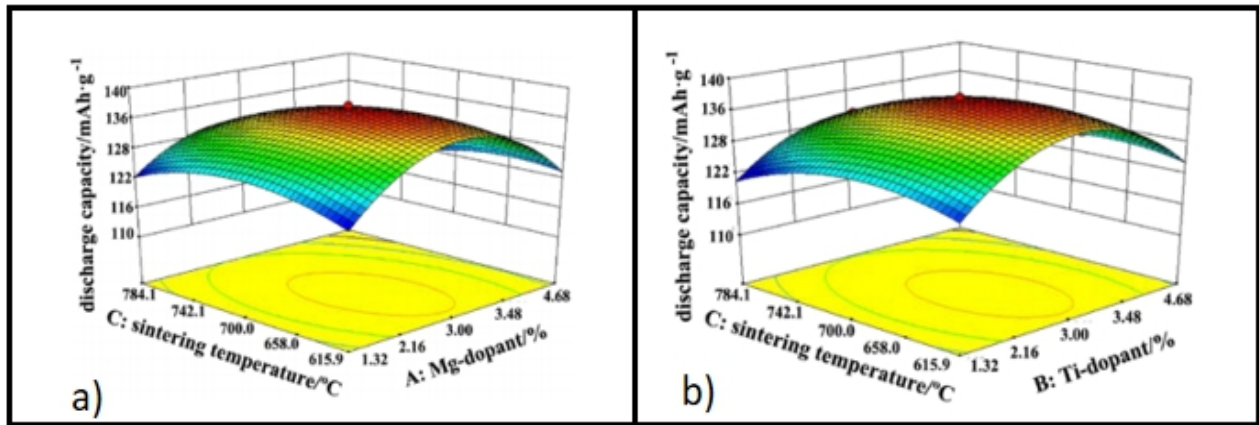


Figure 2.6: Response surface plot for discharge capacity (*Huang et al. 2016*).

Shima Sharifi conducted a simulation on the optimization of the direct methanol fuel cells (DMFC). The aim of this study was to maximize the power density by optimizing the operating parameters using the historical data in response surface methodology. The response which is the power density is affected by three factors which are fuel cell temperature, methanol concentration and oxygen flow rate. The experiments were carried out according to the following ranges: temperature (50-70 °C), methanol concentration (0.5-2 M) and oxygen flow rate of (300-1,000 ml/min). The result shows that the developed mathematical model and all the operating variables are significant. The maximized power density was 38.1 (mW/cm²) at the operating condition of: cell temperature of 70 °C, methanol concentration of 1 M and oxygen flow rate of 300 ml/min (Sharifi et al. 2020). The 3D surface response of the relationship between operating temperature, oxygen flow rate and methanol concentration on the power density is shown in **Figure 2.7**.

Kanin Charoen also optimize the parameters of DMFC in his literature. The objective of this study was to maximize the power density as well. The historical data was run with 100 sets of data

where the independent variables involved are: methanol concentration of (1-8 M), operating temperature of (30-70 °C) and mordenite (MOR) content of (0-10 %). The predicted mathematical model (cubic model) was tally with the experimental result since the R^2 obtained is 0.9460 which is close to 1. It was found that all the three parameters, methanol concentration, operating temperature, and MOR content have significant effect on the response which is the power density. The optimized power density was 40.012 (mW/cm²) at the operating condition of: operating temperature of 70 °C, methanol concentration of 1.35 M and MOR content of 1.47 % (Charoen et al. 2017). The 3D surface response of the relationship between operating temperature, oxygen flow rate and methanol concentration on the power density is shown in **Figure 2.8**

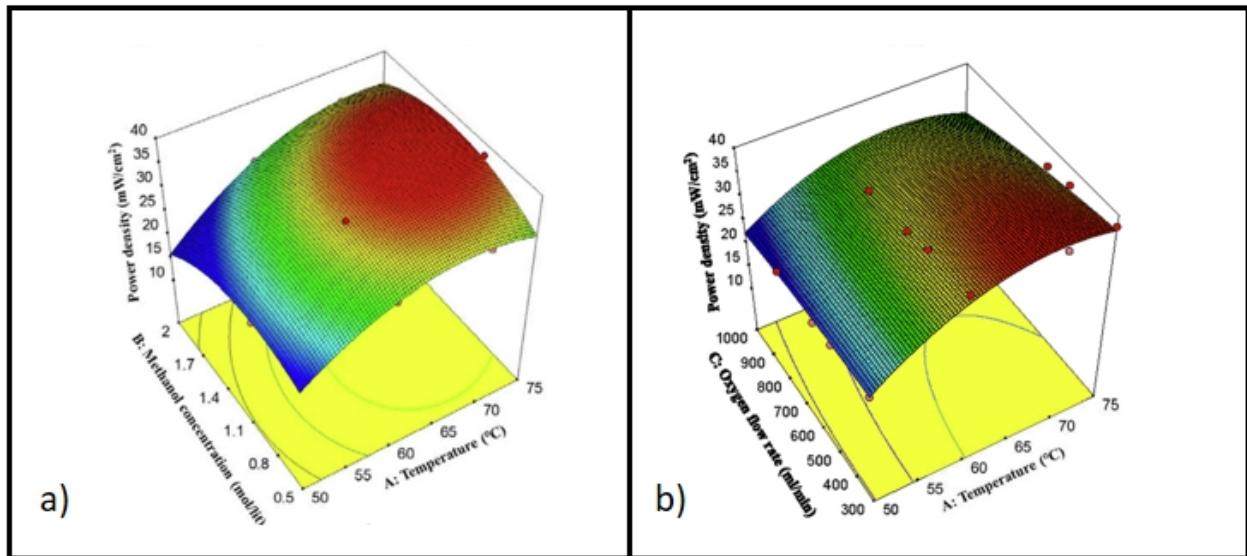


Figure 2.7: Response surface plot for power density ($C_{\text{MEOH}}=1.25$ M, $Q_{\text{O}_2}=300$ ml/min, and $T=70$ °C) (Sharifi et al. 2020).